

A Comprehensive and Detailed Within-Host Modeling Study involving crucial biomarkers and Optimal Drug regimen for Type - I Lepra Reaction : A Deterministic Approach

Dinesh Nayak¹, Bishal Chhetri², D. K. K. Vamsi³, Swapna Muthusamy⁴, and Vijay M. Bhagat⁵

^{1, 2, 3} Department of Mathematics and Computer Science, Sri Sathya Sai Institute of Higher Learning, India.

^{4,5} Central Leprosy Teaching and Research Institute - CLTRI, Chennai, India.

¹First Author. Email: dineshnayak@sssihl.edu.in

³Corresponding author. Email: dkkvamsi@sssihl.edu.in

August 2021

Abstract

Leprosy (Hansen's disease) is an infectious, neglected tropical disease caused by the *Mycobacterium Leprae* (*M. Leprae*). Each year there are approximately 2,02,189 new cases are detected globally. In the year 2017 more than half million people were disabled due to leprosy and almost 50000 new cases are added every year world wide. In leprosy, lepra reactions are the major cause for nerve damage leading to disability. Early detection of lepra reactions through study of biomarkers have important role in prevention of subsequent disabilities. To our knowledge there seems to be very limited literature available on within-host modeling at cellular level involving the crucial biomarkers and the possible optimal drug regimen for leprosy disease and lepra reactions. Motivated by these observations, in this study, we have proposed and analyzed a three dimensional mathematical model to capture the dynamics of susceptible schwann cells, infected schwann cells and the bacterial load based on the pathogenesis of leprosy. We initially have established the existence of solution and later validated the model through the disease characteristics of leprosy. Further we dealt with the local and global stability of different equilibria about the reproduction number value $\mathcal{R}_0 = 1$. Later for numerical studies we estimated the parameters from various clinical papers to make the model more practical. The sensitivity of couple of parameters was evaluated through Partial Rank Correlation Coefficient (PRCC) method to find out the single most influential parameter and also combination of two most influential parameters was studied using Spearman's Rank Correlation Coefficient (SRCC) method. The sensitivity of other remaining parameters was evaluated using Sobol's index. We then have framed and studied an optimal control problem considering the different medication involved in the Multi Drug Therapy (MDT) as control variables. We further studied this optimal control problem along with both MDT and steroid interventions. Finally we did the comparative and effectiveness study of these different control interventions. The finding from this novel and comprehensive study will help the clinicians and public health researchers involved in the process of elimination and eradication of leprosy.

Keywords

Hansen's disease; type - I lepra reaction ; PRCC method; SRCC method; Sobol's Index; MDT; Comparative and effectiveness study

1 Introduction

Leprosy is an infection caused by slow-growing bacteria called *Mycobacterium leprae*. Leprosy is also known as Hansen disease and it is considered to be the oldest disease known to humans. Primarily the bacteria affects the skin and peripheral nerves of the host body. In some of the cases it affects the the mucosa of the upper respiratory tract and the eyes. According to the WHO report [1], global annual number of new cases detected in 2019 was about 2, 02,189. In the year 2017 more than half million people were disabled due to leprosy and almost 50000 are added every year world wide. In leprosy, lepra reactions are the major cause for nerve damage leading to disability. Early detection of lepra reactions through study of biomarkers have important role in prevention of subsequent disabilities.

During the course of the leprosy disease there can be sudden changes in immune-mediated response to *Mycobacterium leprae* antigen which are referred to as leprosy (lepra) reactions. The reactions manifest as acute inflammatory episodes rather than chronic infectious course. There are mainly two types of leprosy reactions. Type 1 reaction is associated with cellular immunity and particularly with the reaction of T helper 1 (Th1) cells to mycobacterial antigens. This reaction involves exacerbation of old lesions leading to the erythematous appearance. Type 2 reaction or erythema nodosum leprosum (ENL) is associated with humoral immunity. It is characterized by systemic symptoms along with new erythematous subcutaneous nodules.

Several clinical and experimental studies has been done on Leprosy. Some works deal about the growth of the *M. Leprae* [2], some on pathogenesis [3]. Now in the context of the mathematical modeling of the disease, there are some contributions that explore the dynamics of transmission of leprosy at population level [4]. In [5] the transmission dynamics of the multibacillary leprosy (MB) and paucibacillary leprosy (PB) including a delay is dealt with. Some works dealing with the cellular level dynamics is explored in [6]. To our knowledge as of date there is no work done yet to explore the dynamics at the level of bio-markers and also there seems to be no mathematical literature available dealing with the optimal drug regimen for treating leprosy and lepra reactions. A mathematical modeling study to this extent will help the clinicians to dissemination of the leprosy by targeting the crucial biomarkers with minimal damage and also helps them for the optimal drug regimen.

Motivated by the above observations, in this study we have proposed and analyzed an within-host three dimensional mathematical model to capture the dynamics of susceptible schwann cells, infected schwann cells and the bacterial load involving the causation biomarkers for type - I lepra reaction based on a detailed flow chart dealing with the pathogenesis of leprosy developed from the clinical works [7–9]. We initially study the natural history of the disease followed studies on the optimal drug regimen for type - I lepra reaction.

The section wise division of this article is as follows. In section 2 we formulate the mathematical model dealing with the type - I lepra reaction based on the pathogenesis of type - I lepra reaction . Later in section 3 we establish the existence, positivity and boudedness of the developed model followed by the local and global stability of different equilibria about the reproduction number

value $\mathcal{R}_0 = 1$ followed by bifurcation analysis. Further in section 4 we numerically depict the theoretical findings of section 3. We validate the proposed model via the leprosy disease characteristics using 2D heat plots in section 5. Further in section 6 we perform the sensitivity analysis of the model parameters. Later in section 7 we do the optimal control studies considering the different medication involved in the Multi Drug Therapy (MDT) as control variables followed by optimal control studies involving both MDT and steroid interventions. Finally we do the comparative and effectiveness study of these different control interventions in section 8. We do the discussion and conclusion in section 9.

Pathogenesis of Leprosy

M. leprae enters through Inhalation

M. leprae adhesins [HLP & HBHA (proteins)] binds to ECM and glycocalyx of epithelial cells.

M. leprae invades host epithelial cells-crosses basement (lower lining of nasal) membrane and connective tissues.

M. leprae enters into the blood stream

M. leprae first encountered by Complements

M. leprae is recognised by toll-like receptors present on the monocytes

M. leprae protein has special affinity towards Schwann cells

Schwann Cells (Nerve Damage)
Through neurovascular bundle (blood vessels)
M. leprae evaginates from blood vessels and comes in close promity to schwann cells

- PGL-1(*M. leprae* protein) affinity to Laminin(protein) of Schwann cells
- Laminin-Laminin binding(protein 2 interaction)
- Disrupts DRP2-dystroglycan complex (this complex is required for myelin formation and information transmission in nerves)

- Infected Schwann cells express MMP 2-9 & TNF alpha
- Degrades ECM(Extracellular Matrix)
- Promotes chronic inflammation-nerve fibre atrophy & irreversible damage

Bacteria increase in number –recognised by the immune system

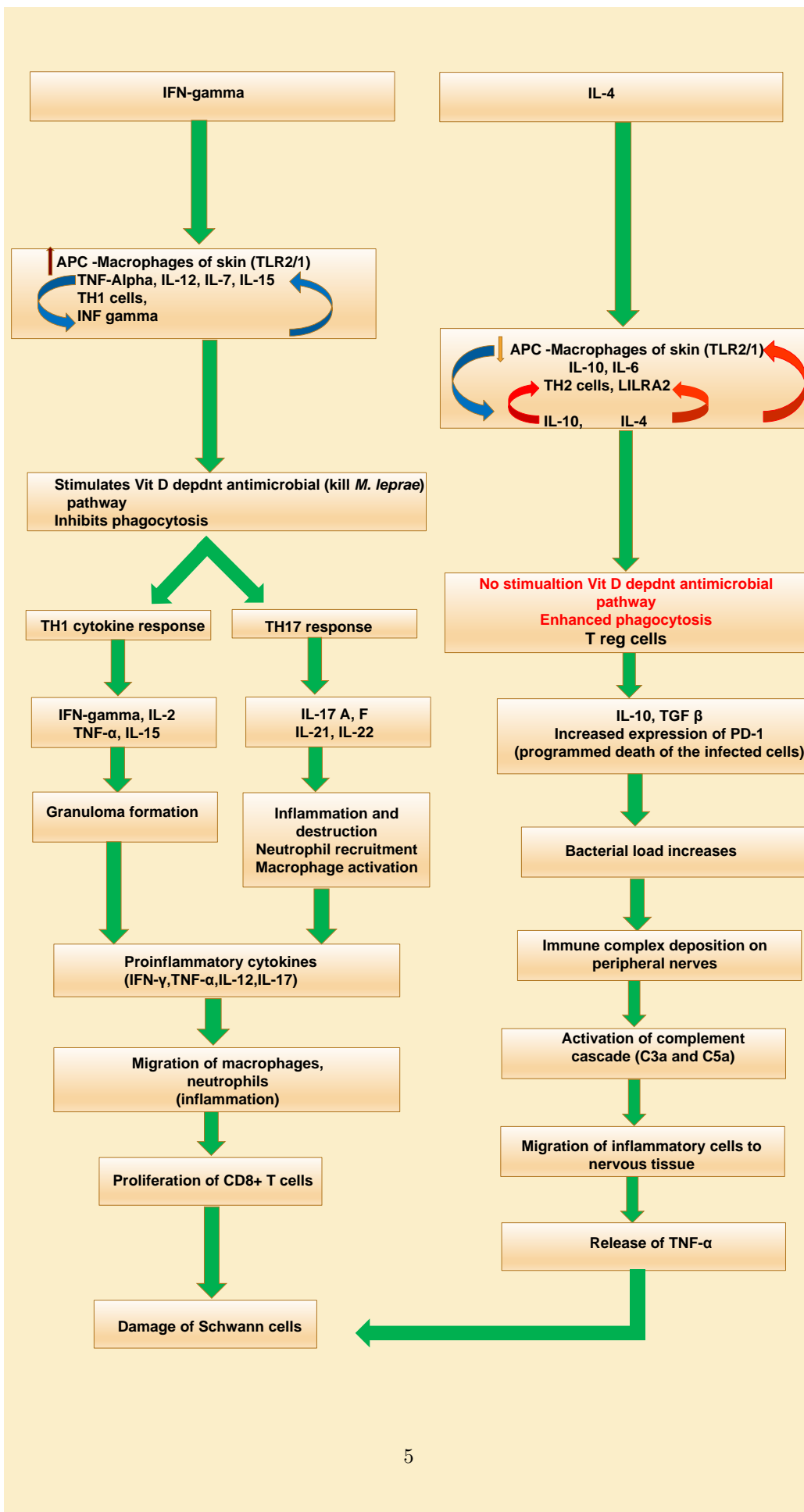
NKT cells and CD4⁺T cells response

TH1 cells (INF gamma dominant)

INF- gamma

TH2 cells (IL-4 gamma dominant)

IL-4



2 mathematical model formulation

Based on the pathogenesis of leprosy dealt in the flow chart earlier we consider a three compartment model dealing with Susceptible schwann cells $S(t)$, Infected schwann cells $I(t)$ and the Bacterial load $B(t)$. We have taken the help of system of ODE's to interpret the biological dynamics in term of mathematical equations.

The dynamics of the susceptible cells i.e. $\frac{dS}{dt}$ will depend on the natural birth rate ω . Also according to the law of mass action the susceptible cell decrease at a rate β hence the term $-\beta SB$. The susceptible cells decrease due the natural death and and the cytokines responses. Next for the dynamics of the infected cells i.e. $\frac{dI}{dt}$ the infected cells increase by βSB and decrease by the natural death and by cytokines responses. The growth of the bacteria depends on the burst rate of the infected cells. Therefore the compartment $\frac{dB}{dt}$ has αI and the bacterial load decreases due to natural death of the bacteria and death due to the cytokines. In summary we propose the following within-host model.

$$\begin{aligned}\frac{dS}{dt} &= \omega - \beta SB - \gamma S - \mu_1 S & (1) \\ \frac{dI}{dt} &= \beta SB - \delta I - \mu_1 I & (2) \\ \frac{dB}{dt} &= \alpha I - (d_{11} + d_{12} + d_{13} + d_{14} + d_{15} + d_{16} + d_{17})B - \mu_2 B & (3)\end{aligned}$$

Symbols	Biological Meaning
S	Susceptible schwann cells
I	Infected schwann cells
B	Bacterila load
ω	Natural birth rate of the susceptible cells
β	Rate at which schwann cells are infected
γ	Death rate of the susceptible cells due to cytokines
μ_1	Natural death rate of schwann cells and infected schwann cells
δ	Death rate of infected schwann cells due to cytokines
α	Burst rate of bacterial particles
$d_{11}, d_{12}, d_{13}, d_{14}, d_{15}, d_{16}, d_{17}$	Rates at which <i>M. Leprae</i> is removed because of the release of cytokines IL-2, IL-7 <i>TNF</i> - α , <i>IFN</i> - γ , IL -12, IL- 15, IL-17 respectively
μ_2	Natural death rate of <i>M. Leprae</i>

3 Stability Analysis

3.1 Positivity and Boundedness

Theorem 1. Positivity: For the model (1) - (3) if initially $S(0) > 0, I(0) > 0$ and $B(0) > 0$ then for all $t \in [0, t_0]$ where $t_0 > 0$, $S(t), I(t), B(t)$ will remain positive in \mathbb{R}_+^3 .

Proof. We now aim to show that for all $t \in [0, t_0]$, $S(t)$, $I(t)$ and $B(t)$ will be positive in \mathbb{R}_+^3 .

Consider

$$\begin{aligned}\frac{dS}{dt} &= \omega - \beta SB - \gamma S - \mu_1 S \\ &\geq -(\beta B - \gamma - \mu_1)S\end{aligned}$$

On solving the above inequality we get

$$\begin{aligned}S(t) &\geq e^{-(\gamma t + \mu_1 t + \int B dt)} > 0 \\ \therefore S(t) &> 0, \forall t \in [0, t_0].\end{aligned}$$

In similar lines we see that

$$\begin{aligned}\frac{dI}{dt} &\geq -\delta I - \mu_1 I \implies I(t) \geq e^{-(\delta + \mu_1)t} > 0 \\ \frac{dB}{dt} &\geq -yB - \mu_2 B \implies B(t) \geq e^{-(y + \mu_2)t} > 0\end{aligned}$$

Here $y = (d_{11} + d_{12} + d_{13} + d_{14} + d_{15} + d_{16} + d_{17})$. Thus for all $t \in [0, t_0]$, $S(t)$, $I(t)$ and $B(t)$ will remain positive i.e. in \mathbb{R}_+^3 . \square

Theorem 2. Boundedness: *There exists an upper bound for each of the variable $S(t)$, $I(t)$, $B(t)$ for all $t \in [0, t_0]$.*

Proof. Let us consider

$$\begin{aligned}\frac{dS}{dt} + \frac{dI}{dt} &= \omega - (\gamma + \mu_1)S - (\delta + \mu_1)I \\ \implies \frac{d(S + I)}{dt} &\leq \omega - \min\{(\gamma + \mu_1), (\delta + \mu_1)\}(S + I)\end{aligned}$$

Considering $k = \min\{(\gamma + \mu_1), (\delta + \mu_1)\}$ and integrating the above we get,

$$(S + I)(t) \leq \frac{\omega}{k} + c_1 e^{-kt}$$

Hence

$$\limsup_{t \rightarrow \infty} (S + I) \leq \limsup_{t \rightarrow \infty} \left(\frac{\omega}{k} + c_1 e^{-kt} \right) = \frac{\omega}{k} < \infty$$

$\therefore (S + I)(t)$ is bounded thus $S(t)$, $I(t)$ are bounded. Since

$$S(t), I(t) \leq (S + I)(t)$$

Now for $t \in [0, t_0]$, there exist S_{max} and I_{max} such that $S(t) \leq S_{max}$, $I(t) \leq I_{max}$.

We now consider $\frac{dB}{dt} = \alpha I - (y + \mu_2)B$.

Solving the above differential equation for $B(t)$, we get,

$$\begin{aligned}Be^{(y + \mu_2)t} &= \int \alpha I e^{(y + \mu_2)t} dt \\ &\leq \int \alpha \frac{\omega}{k} e^{(y + \mu_2)t} dt \\ &= \frac{\alpha \omega}{k(y + \mu_2)} e^{(y + \mu_2)t} + c_2 \\ \implies B(t) &\leq \frac{\alpha \omega}{k(y + \mu_2)} + c_2 e^{-(y + \mu_2)t}\end{aligned}$$

$$\therefore \limsup_{t \rightarrow \infty} B(t) \leq \limsup_{t \rightarrow \infty} \left(\frac{\alpha\omega}{k(y + \mu_2)} + c_2 e^{-(y + \mu_2)t} \right) = \frac{\alpha\omega}{k(y + \mu_2)} < \infty$$

Hence there exists an upper bound for $B(t)$, say B_{max} for $t \in [0, t_0]$.

Hence $S(t)$, $I(t)$ and $B(t)$ all are bounded for $t \in [0, t_0]$. \square

3.2 Existence of the solution

Theorem 3. *Let $t_0 > 0$. If the model (1) - (3) initially satisfies $S(0) > 0$, $I(0) > 0$ and $B(0) > 0$ then $\forall t > 0$ there exists a unique solution for the system in \mathbb{R}_+^3 .*

Proof. The system (1) - (3) in the vectorial form is given by

$$\frac{dX}{dt} = f(X)$$

where

$$X = \begin{bmatrix} S(t) \\ I(t) \\ B(t) \end{bmatrix} \text{ and } f(X) = \begin{bmatrix} \omega - \beta SB - \gamma S - \mu_1 S \\ \beta SB - \delta I - \mu_1 I \\ \alpha I - yB - \mu_2 B \end{bmatrix}$$

Now we can see that $f(X) : \mathbb{R}^3 \rightarrow \mathbb{R}^3$ has continuous derivative and thus it's locally lipschitz in \mathbb{R}^3 . Hence from fundamental existence and uniqueness theorem [10, 11], we can conclude the existence of unique solution for the system (1) - (3). \square

3.3 Equilibrium points and the reproduction number (\mathcal{R}_0)

The basic reproduction number for the system (1) - (3) is calculated using the next generation matrix method [12] and the expression for \mathcal{R}_0 is found to be

$$\mathcal{R}_0 = \frac{\alpha\beta\omega}{(\gamma + \mu_1)(\delta + \mu_1)(y + \mu_2)}.$$

We also see that the system (1) - (3) admits two equilibria namely, the infection/disease free equilibrium $E_0 = \left(\frac{\omega}{\mu_1}, 0, 0 \right)$ and the infected equilibrium $E^* = (S^*, I^*, B^*)$, where

$$\begin{aligned} S^* &= \frac{(\delta + \mu_1)(y + \mu_2)}{\alpha\beta} = \frac{\omega}{(\gamma + \mu_1)\mathcal{R}_0} \\ I^* &= \frac{\alpha\beta\omega - (\gamma + \mu_1)(\delta + \mu_1)(y + \mu_2)}{\alpha\beta(\delta + \mu_1)} = \frac{(\gamma + \mu_1)(y + \mu_2)(\mathcal{R}_0 - 1)}{\alpha\beta} \\ B^* &= \frac{\alpha\beta\omega - (\gamma + \mu_1)(\delta + \mu_1)(y + \mu_2)}{\beta(\delta + \mu_1)(y + \mu_2)} = \frac{(\gamma + \mu_1)(\mathcal{R}_0 - 1)}{\beta} \end{aligned}$$

3.4 Stability Analysis of E_0

Local Stability:

In the following we do the local stability analysis of the infection free equilibrium E_0 .

The Jacobian matrix of the system at the infection free equilibrium E_0 is given by,

$$J_{E_0} = \begin{pmatrix} -(\gamma + \mu_1) & 0 & \frac{-\beta\omega}{(\gamma + \mu_1)} \\ 0 & -(\delta + \mu_1) & \frac{\beta\omega}{(\gamma + \mu_1)} \\ 0 & \alpha & -(y + \mu_2) \end{pmatrix}$$

The characteristic equation is given by,

$$\left(-(\gamma + \mu_1) - \lambda \right) \left[\lambda^2 + \{(\gamma + \mu_1) + (y + \mu_2)\} \lambda + (\gamma + \mu_1)(y + \mu_2) - \frac{\beta \alpha \omega}{(\gamma + \mu_1)} \right] = 0 \quad (4)$$

One of the eigenvalues of the above equation is $\lambda_1 = -(\gamma + \mu_1)$ which is less than zero and the other two eigenvalues are calculated as follows:

Introducing \mathcal{R}_0 in the rest part of the equation

$$\lambda^2 + \{(\gamma + \mu_1) + (y + \mu_2)\} \lambda + (\gamma + \mu_1)(y + \mu_2)(1 - \mathcal{R}_0) = 0 \quad (5)$$

Letting $A(\gamma + \mu_1) + (y + \mu_2)$ and $D = (\gamma + \mu_1)(y + \mu_2)$ the roots of the above equation are given by

$$\lambda = \frac{1}{2} \left[-A \pm \sqrt{A^2 + 4(\mathcal{R}_0 - 1)D} \right]$$

We now consider the following two cases for understanding the stability of infection free equilibrium.

Case I: When $\mathcal{R}_0 < 1$

Further in this case we need to consider the following two sub cases:

(a) $A^2 + 4(\mathcal{R}_0 - 1)D > 0$

(b): $A^2 + 4(\mathcal{R}_0 - 1)D < 0$

Sub-case (a): When $A^2 + 4(\mathcal{R}_0 - 1)D > 0$ then the eigenvalues are given by,

$$\lambda_{2,3} = A \pm \sqrt{A^2 + 4(\mathcal{R}_0 - 1)D}$$

which are less than zero.

Therefore the infection free equilibrium point E_0 is asymptotically stable in this case as all the eigenvalues are negative.

Sub-case (b): When $A^2 + 4(\mathcal{R}_0 - 1)D < 0$ the eigenvalues are complex conjugates with the negative real parts. Therefore in this case also we have E_0 to be asymptotically stable.

Hence we conclude that E_0 is locally asymptotically stable (LAS) whenever $\mathcal{R}_0 < 1$.

Case II: When $\mathcal{R}_0 > 1$

In this case the characteristic equation has two negative eigenvalues and one positive eigenvalue. Hence whenever $\mathcal{R}_0 > 1$ the infection free equilibrium E_0 becomes unstable.

Global Stability:

As in *Andrei Korobeinikov* [13], we consider the *Lyapunov function* of the system (1) - (3) as

$$U(S, I, B) = S_0 \left(\frac{S}{S_0} - \ln \frac{S}{S_0} \right) + I + \frac{(\delta + \mu_1)}{\alpha} B$$

Now

$$\frac{dU}{dt} = \omega \left(2 - \frac{S}{S_0} - \frac{S_0}{S} \right) + \frac{(\delta + \mu_1)(y + \mu_2)}{\alpha} (\mathcal{R}_0 - 1) B$$

Here $\left(2 - \frac{S}{S_0} - \frac{S_0}{S} \right) < 0$ and for $\mathcal{R}_0 < 1$, the derivative $\frac{du}{dt} < 0$.

\therefore For $\mathcal{R}_0 < 1$ the disease free equilibrium E_0 is Globally Asymptotically Stable (GAS).

3.5 Stability Analysis of E^*

Local Stability:

The Jacobian matrix of the system for E^* is given by

$$J = \begin{pmatrix} -(\gamma + \mu_1)\mathcal{R}_0 & 0 & -\frac{(\delta + \mu_1)(y + \mu_2)}{\alpha} \\ (\gamma + \mu_1)(\mathcal{R}_0 - 1) & -(\delta + \mu_1) & \frac{(\delta + \mu_1)(y + \mu_2)}{\alpha} \\ 0 & \alpha & -(y + \mu_2) \end{pmatrix}$$

The characteristic equation of the Jacobian J evaluated at E^* is given by,

$$\lambda^3 + \left(p + (\gamma + \mu_1)\mathcal{R}_0\right)\lambda^2 + \left(p(\gamma + \mu_1)\mathcal{R}_0\right)\lambda + q(\gamma + \mu_1)(\mathcal{R}_0 - 1) = 0$$

where $p = (\gamma + \mu_1)(y + \mu_2)$ and $q = (\gamma + \mu_1)(y + \mu_2)$.

Since $\mathcal{R}_0 > 1$, $(p + (\gamma + \mu_1)\mathcal{R}_0) > 0$, $(p(\gamma + \mu_1)\mathcal{R}_0) > 0$ and $q\mu_1(\mathcal{R}_0 - 1) > 0$. Therefore if we substitute $\lambda = -\lambda$ in the above characteristic equation, we get all the roots of equation to be negative from Descartes rule of sign change. Hence we conclude that the infected equilibrium point E_1 exists and remains asymptotically stable whenever $\mathcal{R}_0 > 1$.

Global Stability:

Considering the *Lyapunov function* of the system (1) - (3) for E^* as in [13]

$$U^*(S, I, B) = S^* \left(\frac{S}{S^*} - \ln \frac{S}{S^*} \right) + I^* \left(\frac{I}{I^*} - \ln \frac{I}{I^*} \right) + \frac{(\delta + \mu_1)}{\alpha} B^* \left(\frac{B}{B^*} - \ln \frac{B}{B^*} \right)$$

we can show the GAS of E^* when $\mathcal{R}_0 > 1$.

3.6 Bifurcation Analysis

We now use the method given by *Bruno Buonomo* in [14] to do the bifurcation analysis for the system (1) - (3).

Theorem 4. *The system (1) - (3) undergoes a trans-critical bifurcation at $\mathcal{R}_0 = 1$ and it is forward.*

Proof. Let's consider $x_1 = I, x_2 = B, x_3 = S$ and $x = (x_1, x_2, x_3)$.

Now

$$\begin{aligned} \text{Infected_class} \begin{cases} \frac{dx_1}{dt} &= \beta x_2 x_3 - (\delta + \mu_1)x_1 \\ \frac{dx_2}{dt} &= \alpha x_1 - (y + \mu_2)x_2 \end{cases} \\ \text{Uninfected_class} \begin{cases} \frac{dx_3}{dt} &= \omega - \beta x_2 x_3 - (\gamma + \mu_1)x_3 \end{cases} \end{aligned}$$

We consider $f(x) = (f_1, f_2, f_3) = \left(\frac{dx_1}{dt}, \frac{dx_2}{dt}, \frac{dx_3}{dt} \right)$, hence $f(x)$ is twice differentiable function in \mathbb{R}^3 .

Further we can interpret each f_i as

$$f_i(x) = \mathcal{F}_i(x) - \mathcal{V}_i(x), \quad i = 1, 2, 3$$

Where $\mathcal{V}_i = V_i^- - V_i^+$ and here

- \mathcal{F}_i := Appearance rate of new infection in i^{th} compartment
- \mathcal{V}_i^+ := Transfer rate of individuals **into** the i^{th} compartment.
- \mathcal{V}_i^- := Transfer rate of individuals **out of** the i^{th} compartment.

Therefore here

- $\mathcal{F}_1 = \beta x_2 x_3, \mathcal{V}_1^+ = 0, \mathcal{V}_1^- = (\delta + \mu_1)x_1$
- $\mathcal{F}_2 = \alpha x_2, \mathcal{V}_2^+ = 0, \mathcal{V}_2^- = (y + \mu_2)x_2$
- $\mathcal{F}_3 = 0, \mathcal{V}_3^+ = 0, \mathcal{V}_3^- = \beta x_2 x_3 + (\gamma + \mu_1)x_3$

Denote \mathcal{X}_s as the set of all disease free state i.e.

$$\mathcal{X}_s := \{x \in \mathbb{R}^3 : x_1 = 0, x_2 = 0\} = \left\{ \left(0, 0, \frac{\omega}{(\gamma + \mu_1)} \right) \right\}$$

Now we will satisfy the condition **A1 - A5** of [14] as follows

A1: All $\mathcal{F}_i, \mathcal{V}_i^+$ and \mathcal{V}_i^- are positive for $i = 1, 2, 3$ in the nonnegative cone $\{x \in \mathbb{R} : x_i \geq 0, i = 1, 2, 3\}$

A2: If $x \in \mathcal{X}_s$ then $\mathcal{V}_i^- = 0$ for the infected compartment, i.e. $i = 1, 2$. Since for $x \in \mathcal{X}_s$ we have $x_1 = 0$ and $x_2 = 0$

$$\implies \mathcal{V}_1^- = (\delta + \mu_1).0 = 0, \mathcal{V}_2^- = (y + \mu_2).0 = 0$$

A3: No incidence of infection in uninfected compartment(x_3), that is $\mathcal{F}_3 = 0$

A4: Disease free subspace is invariant, that means for $x \in \mathcal{X}_s$, here $\mathcal{F}_i = 0, \mathcal{V}_i^+ = 0, i = 1, 2$

A5: Now putting all $\mathcal{F}_i = 0$, we have

$$f(x) = (-(\delta + \mu_1)x_1, -(y + \mu_2)x_2, \omega - \beta x_2 x_3 - (\gamma + \mu_1)x_3)$$

Now the derivative matrix of $f(x)$ is given by

$$\begin{aligned} \mathcal{D}_{f(x)} &= \begin{bmatrix} -(\delta + \mu_1) & 0 & 0 \\ 0 & -(y + \mu_2) & 0 \\ 0 & \beta x_3 & -\beta x_2 - (\gamma + \mu_1) \end{bmatrix} \\ \implies \mathcal{D}_{f(x_0)} &= \begin{bmatrix} -(\delta + \mu_1) & 0 & 0 \\ 0 & -(y + \mu_2) & 0 \\ 0 & \frac{-\beta\omega}{(\gamma + \mu_1)} & -(\gamma + \mu_1) \end{bmatrix} \end{aligned}$$

where $x_0 \in \mathcal{X}_s$, and here $\mathcal{D}_{f(x_0)}$ is a lower triangular matrix with all negative diagonal entries and hence all the eigen values illustrating that the disease free equilibrium is stable in the absence of new infections.

We now show that the following hypothesis **H1 - H3** of [14], is also satisfied.

H1: The only nonlinear term present in infected compartment of the system is $\mathcal{F}_1 = \beta x_2 x_3$

H2: Let $T(x_2, x_3) = \beta x_2 x_3$

- $T(kx_2, x_3) = \beta k.x_2x_3 = k.\beta x_2x_3 = k.T(x_2, x_3)$
- $T(x_2, kx_3) = \beta x_2.kx_3 = k.\beta x_2x_3 = k.T(x_2, x_3)$
- $T(x_2 + x'_2, x_3) = \beta(x_2 + x'_2)x_3 = \beta x_2x_3 + \beta x'_2x_3 = T(x_2, x_3) + T(x'_2, x_3)$
- $T(x_2, x_3 + x'_3) = \beta x_2(x_3 + x'_3) = \beta x_2x_3 + \beta x_2x'_3 = T(x_2, x_3) + T(x_2, x'_3)$

∴ The nonlinear term in the above hypothesis (**H1**) is bilinear in nature.

H3: There is no transfer from infected compartment to uninfected compartment.

Now using *Proposition-1* in the paper [14] we can conclude that the system (1) - (3) undergoes a trans-critical bifurcation at $\mathcal{R}_0 = 1$ which is forward in nature. \square

4 Numerical Simulations

All the values of the parameters used here are estimated from different clinical papers. The appropriate references are cited in the Table 1. Some parameters are minimally fine tuned from the Table 1 values to satisfy certain hypothesis assumptions in some of the following plots.

Symbols	Values	Units
ω	0.022 [15]	day^{-1}
β	3.44 [16]	day^{-1}
γ	0.1795 [17]	day^{-1}
μ_1	0.0018 [17]	day^{-1}
δ	0.2681 [17]	day^{-1}
α	0.063 [18]	day^{-1}
y	0.0003 [6]	day^{-1}
μ_2	0.57 [19]	day^{-1}

Table 1: Values of the parameters complied from clinical literature

4.1 Disease free equilibrium E_0

We now depict the local and global stability of the disease free equilibrium E_0 . Figures 1a and 1b depict the local and global stability of E_0 .

We choose parameters in Table 2 in such a way that $\mathcal{R}_0 = 0.9939 < 1$ and for these parameters we have $E_0 = (55.1899, 0, 0)$. For depicting the global stability of E_0 we have arbitrarily considered the solution trajectories taking ten different initial conditions.

ω	β	γ	μ_1	δ	α	y	μ_2
1.090	0.44	0.01795	0.0018	0.2681	0.0063	0.0003	0.57

Table 2: Values of the parameters taken for E_0

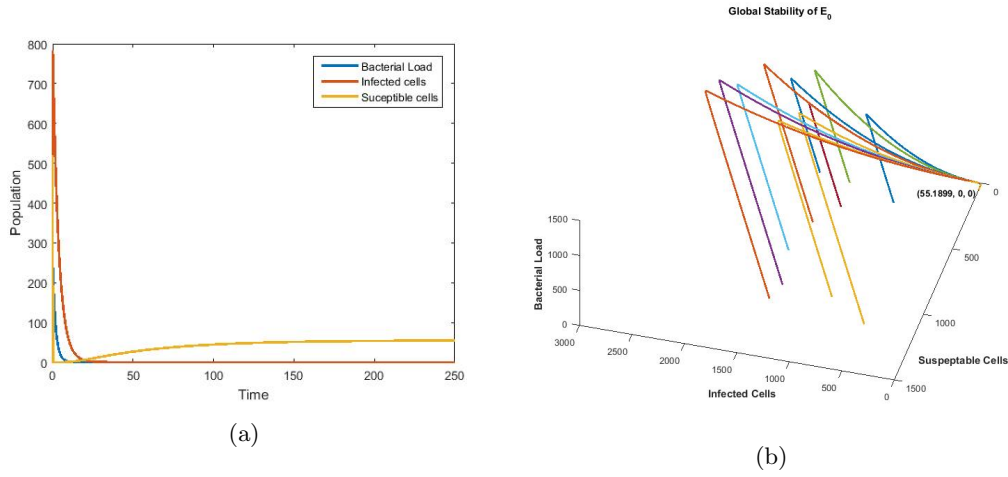


Figure 1: Local and global Stability of the system (1) - (3) at E_0

4.2 Infected/endemic equilibrium E^*

We now depict the local and global stability of the endemic equilibrium E^* . Figures 2a and 2b depict the local and global stability of E^* .

For the numerical simulations we have chosen the values of parameters as in Table 3. For these parameter values we have $\mathcal{R}_0 = 29.6341 > 1$ and the $E^* = (38.9006, 75.2748, 17.3046)$. For depicting the global stability of E^* we have arbitrarily considered solution trajectories with different initial conditions.

ω	β	γ	μ_1	δ	α	y	μ_2
20.90	0.030	0.01795	0.00018	0.2681	00.2	0.3	0.57

Table 3: Values of the parameters taken for E^*

4.3 Transcritical Bifurcation

In this bifurcation there is an exchange of stability between E_0 and E^* as \mathcal{R}_0 crosses unity. To depict this bifurcation, we varied the parameter ω from 0 to 0.25 with step size 0.001 and chose the other parameters from Table 1. The Figure 3 depicts the occurrence of Transcritical bifurcation at $\mathcal{R}_0 = 1$.

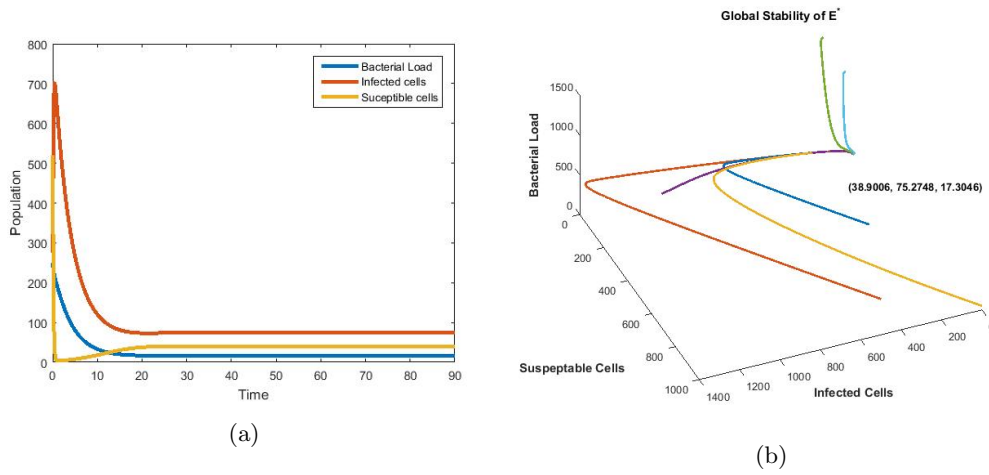


Figure 2: Local and global stability of the system (1) - (3) at E^* .

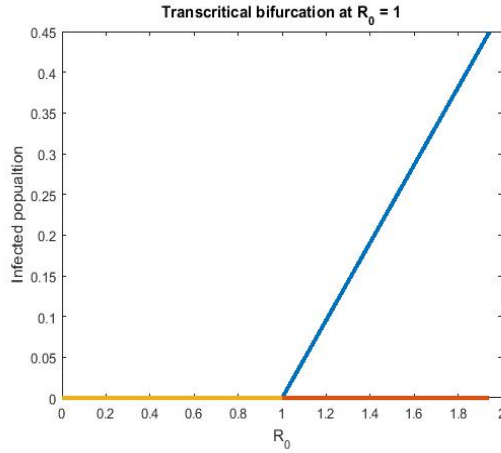


Figure 3: Figure depicting the transcritical bifurcation exhibited by the system (1) - (3) at $R_0 = 1$

5 Model validation through 2D Heat Plots

Form some of the clinical studies we see that the average doubling time of the *M. Leprae* is approximately 14 days [20]. Based on this characteristic, we now validate the model (1) - (3) through 2D heat plot.

We now vary the parameters α from 0.2263 to 0.3099 on the x -axis and the parameter γ between 0.15 to 0.2090 on the y -axis and generate a two parameter heat plot to validate our model (1) - (3). All other parameter are taken from Table 1 and the initial condition was chosen to be $(S_0, I_0, B_0) = (5200, 0, 40)$.

Now from the Figure 4 it can be seen that the proposed model is able to reproduce characteristic, i.e. exactly the double of initial count of bacterial load that is 80 ($B_0 = 40$), indicated by the dotted red rectangle.

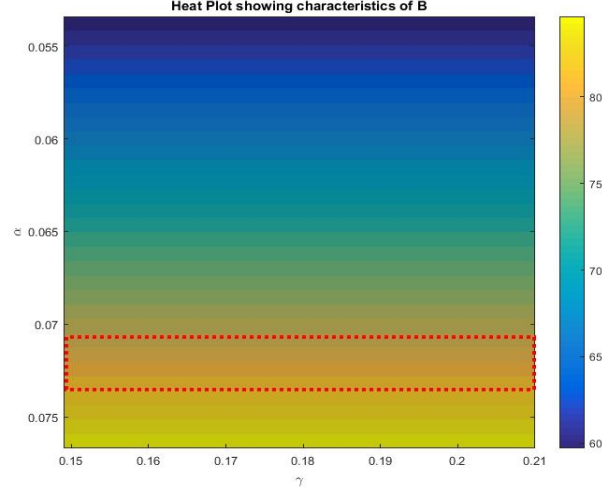


Figure 4

6 Sensitivity Analysis

Here we are interested in investigating the impact of uncertainty in the values of the different parameters on the variables (S, I, B) . For this we have used the Global Sensitivity Analysis (GSA) methodology through Latin hyper cube sampling (LHS). LHS is a technique that involves sampling without replacement a set of model parameter combinations from preset ranges on the parameter values [21–23]. Using this sample we generate the scatter plot to decide the methodology for GSA. The scatter plots enables the graphical detection of the non-linearities, non-monotonicities between model input (parameter) and output (variables). If the trend is non-linear then rank correlation coefficient such as Partial Rank Correlation Coefficient (PRCC), Spearman’s Rank Correlation Coefficient (SRCC) will be used for further sensitivity analysis where as if the trend is non-monotonic, method based on decomposition of model output variance such as Sobol’s method will be the best choice for further analysis.

6.1 LHS and Scatter plots

As an initial step to LHS we select the following parameters listed in Table 4 having possible uncertainty in their values and consider them for the process of sampling. The range of the variable values used for sampling is listed in Table 4. All the parameter value ranges are chosen based on the clinical papers [17, 18] and we introduced an uncertainty in y for our computational convenience. The remaining values of the parameters are as in Table 1.

Then the LHS is done to create 1000 sets of parameter sample each containing 5 random values of parameters. Now each set of these parameters was used to simulate the model at each time. Scatter plots were created for each parameter vs variable to decide the further procedure of GSA.

In the Figure 5 we can easily see that the relationships between δ and all variables such as $S(t)$, $I(t)$ and $B(t)$ follow a monotonic trend and the so is the case for y . Therefore we did the SRCC and PRCC for these two variable and the remaining parameters were analysed by calculating the Sobol’s index.

Parameter	Max Value	Min Value
γ	0.0763	0.0538
μ_1	0.0405	0.0305
δ	0.3099	0.2263
α	0.0763	0.0538
y	0.0001	0.0005

Table 4: Range of sensitive parameters

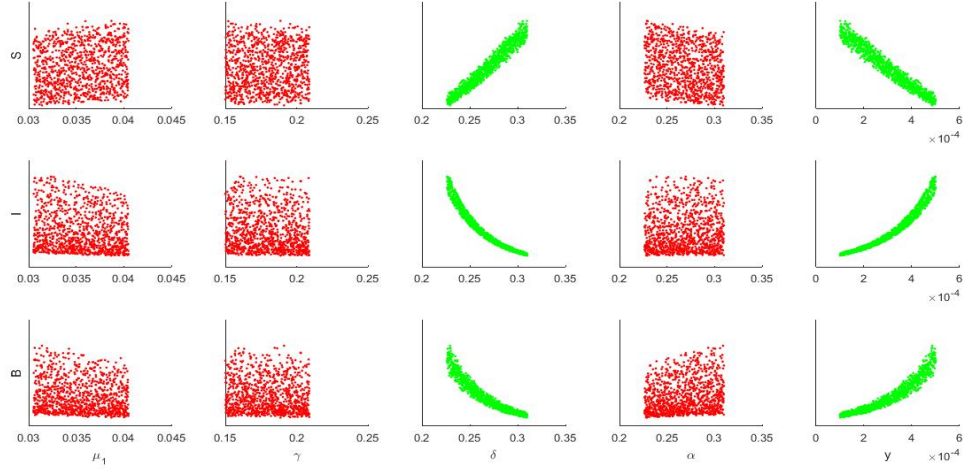


Figure 5: Scatter plots for parameters vs variables such as $S(t)$, $I(t)$ and $B(t)$

6.2 SRCC and PRCC

Using the same sample obtained above, we calculated SRCC index separately for δ and y and the PRCC index jointly.

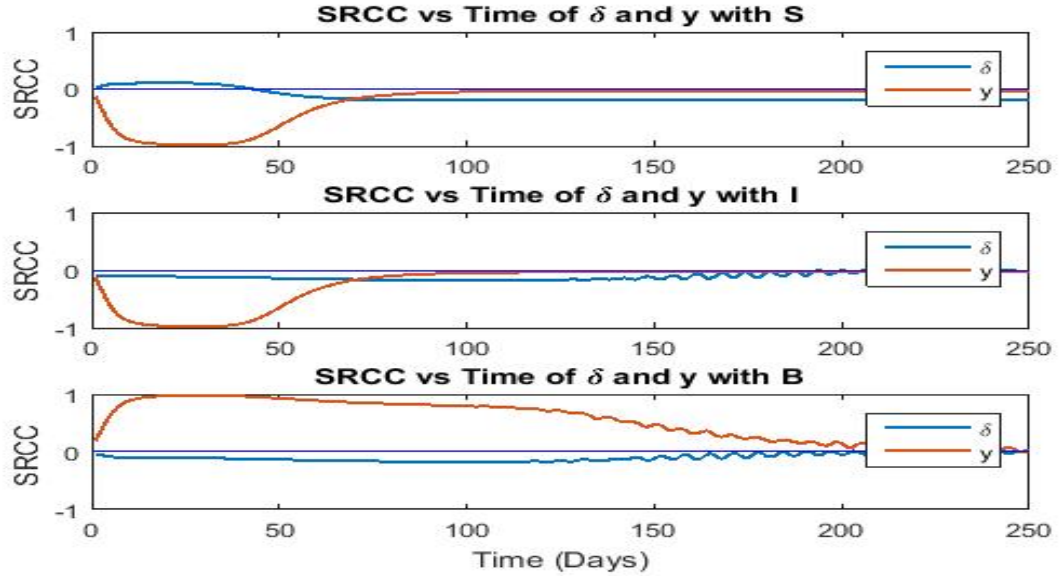


Figure 6: Plot for SRCC with respect to time

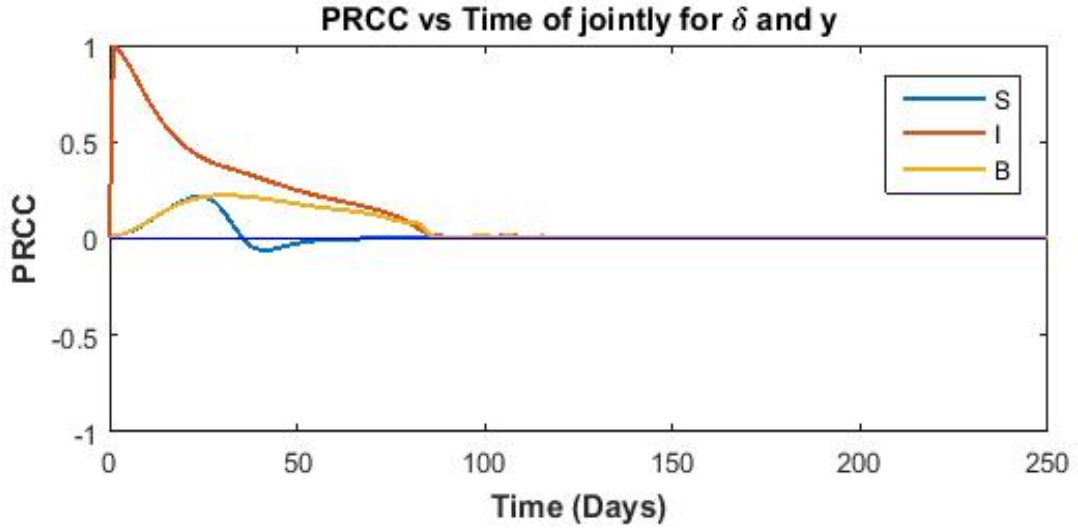


Figure 7: Plot for PRCC with respect to time

The Figure 6 shows that δ has more negative impact on S and I in comparison to y , whereas y has more positive impact on B . The $PRCC$ plot 7 shows that the cumulative impact of δ and y seems to be more on the Infected cell population I .

6.3 Sobol's Index

The Sobol's index is calculated using the formula of correlation [24].

$$S_i = Corr(Y, E(Y/x_i))$$

where S_i is the Sobol's index of i^{th} parameter, Y is the model output value and $E(Y/x_i)$ conditional expectation/ mean of model output Y .

The Sobol's index was calculated for the parameters μ_1, γ, α at each time as in SRCC and was plotted separately for the model variables S, I and B which can be seen in Figure 8. Unfortunately from these plots any we couldn't derive fruitful conclusions to decide the most sensitive parameter owing to the high fluctuations.

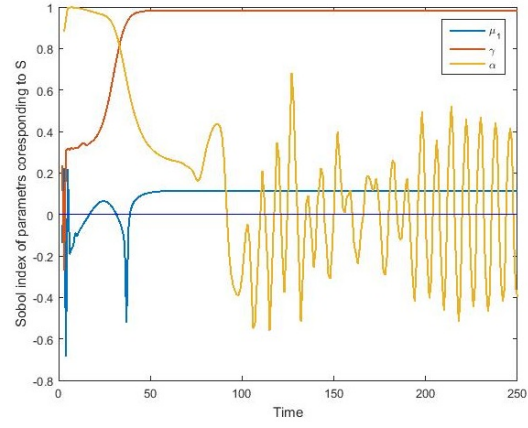
Because of the above limitation we tried to identify the sensitive parameters with respect to \mathcal{R}_0 which is discussed in next section.

6.4 Sensitivity of \mathcal{R}_0

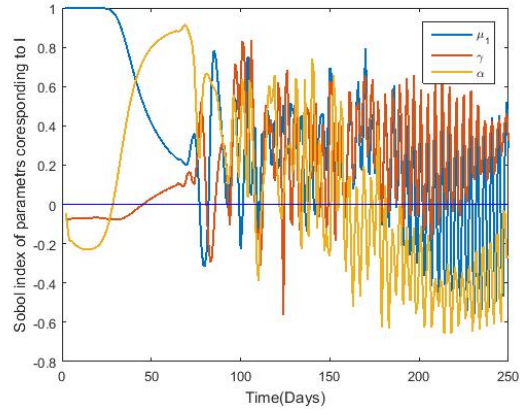
For identifying the sensitive parameters with respect to \mathcal{R}_0 , we did the scatter plots of the parameters against \mathcal{R}_0 and saw that none of them were qualified for PRCC analysis. Hence we calculated the Sobol's sensitivity index for each parameter and pairs of parameters as listed in frames of the plot 9.

6.5 Inference

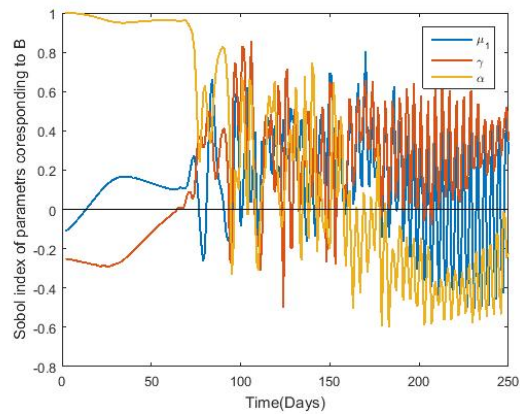
From the above sensitivity analysis we can conclude that α is the most sensitive parameter followed by δ and y . Here α and δ have direct impact on the system where as y has inverse impact on the system as it has a negative Sobol's index. In case of cumulative parameter sensitivity we see that the parameter combination of α and δ is the most sensitive combination that impacts the system (1) - (3).



(a)



(b)



(c)

Figure 8: Plot of Sobol's index of μ_1 , γ and α with S, I and B respectively

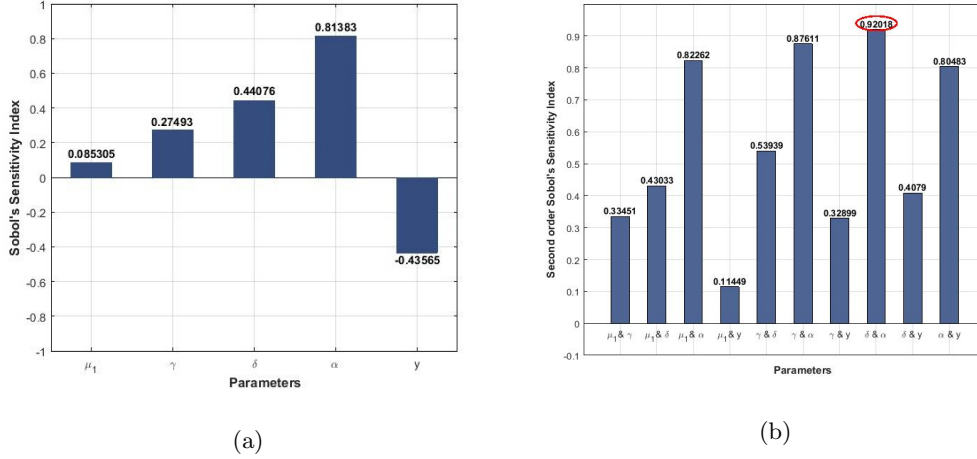


Figure 9: Sensitivity through Sobol's Index with respect to \mathcal{R}_0 as output

7 Optimal Control Studies

Presently for the type - I lepra reaction two kinds of medication are prescribed based on the disease condition [25, 26]. Firstly Multi Drug Therapy (MDT) is used and in case still the reaction burden doesn't reduce, then steroids are given along with MDT treatment.

Motivated by the above clinical findings in this section we frame and study two optimal control problems. First one deals with the optimal drug regimen for MDT and the second deals with the optimal drug regimen for the scenario involving both MDT and steroid interventions. These medical/drug interventions are modeled as control variables for the system (1) - (3).

7.1 Optimal control problem associated with MDT

According to the WHO recommended guidelines of 2018 for Leprosy MDT consist of three drugs *Rifampin*, *Dapsone* and *Clofazimine* [25, 27]. The drug rifampin acts as a rapid bacillary killer and thereby indirectly reduces the amount of cells getting infected. Therefore the control variable $D_{12}(t)$ is negatively incorporated in the infected cell compartment of (7) - (9) and $D_{13}^2(t)$ is negatively incorporated in the bacterial load compartment of (7) - (9). Here the square on $D_{13}(t)$ is used for capturing the extent of intense action of this drug on bacterial load. The drug dapsone is bactericidal and bacteriostatic against *M. leprae* and it also has some adverse effect of nerve damage due to the cytokines responses [28]. To capture this action of the drug we incorporate $D_{21}(t)$ and $D_{22}(t)$ in the compartments S and I of (7) - (9) and $D_{23}^2(t)$ in the B compartment of (7) - (9). The third drug clofazimine has an immuno-suppressive effect and also it binds with DNA of the bacteria causing the inhibition of template function of DNA resulting bacteriostatic against *M. leprae* [29]. To incorporate this phenomenon we add the control variable $D_{31}(t)$ to the S compartment in (7) - (9) resulting increase of these cells. $D_{33}(t)$ is negatively incorporated in the B compartment of (7) - (9) to indicate the inhibition of bacterial replication.

Now mathematically we define the set of all control variables as follows:

$$U = \left\{ D_{ij}(t), D_{ij}(t) \in [0, D_{ij}max], 1 \leq i, j \leq 3, ij \neq 32, t \in [0, T] \right\}$$

Here $D_{ij}max$ represents the maximum value of the corresponding control variable which depends on the availability and limit of the drugs recommended for patients and T is the final time

of observation.

Since the drugs used in MDT can be toxic and can lead to side effects for solving this optimal control problem we consider a cost functional that minimizes the drug concentrations along with the infected cell count and bacterial load. Based on this we consider the following cost functional:

$$\mathcal{J}_{min}(D_1, D_2, D_3) = \int_0^T \left(I(t) + B(t) + P[D_{11}^2(t) + D_{12}^2(t) + D_{13}^3(t)] + Q[|D_2|^2] + R[|D_3|^2] \right) dt \quad (6)$$

subject to the constraints/system

$$\frac{dS}{dt} = \omega - \beta SB - \gamma S - \mu_1 S - D_{11}(t)S - D_{21}(t)S + D_{31}(t)S \quad (7)$$

$$\frac{dI}{dt} = \beta SB - \delta I - \mu_1 I - D_{12}(t)I - D_{22}(t)I \quad (8)$$

$$\frac{dB}{dt} = (\alpha - D_{23}^2(t) - D_{33}(t))I - yB - \mu_2 B - D_{13}^2(t)B \quad (9)$$

Here $D_1 = (D_{11}, D_{12}, D_{13})$, $D_2 = (D_{21}, D_{22}, D_{23})$, $D_3 = (D_{31}, D_{33})$ and $|\bullet|$ represents standard Euclidean norm in \mathbb{R}^n and $(D_1, D_2, D_3) \in U$.

The integrand of the cost function 6, denoted by

$$L(I, V, D_1, D_2, D_3) = \left(I(t) + B(t) + P[D_{11}^2(t) + D_{12}^2(t) + D_{13}^3(t)] + Q[|D_2|^2] + R[|D_3|^2] \right) \quad (10)$$

is the lagrangian or running cost of the optimal control problem.

The admissible set of solutions for the above optimal control problem (6) - (9) is given by

$$\Omega = \left\{ (I, V, D_1, D_2, D_3) : I, V \text{ satisfying (7) - (9)} \forall (D_1, D_2, D_3) \in U \right\}$$

7.2 Existence of optimal solution

In the section we establish the existence of optimal control for the system (6) - (9) using the existence theorem 2.2 of [30] dealing with nonlinear control systems.

Theorem 5. *There exists a 8- tuple of optimal controls $(D_1^*(t), D_2^*(t), D_3^*(t))$ in the set of admissible controls U such that the cost function is minimized i.e.*

$$\mathcal{J}(D_1^*(t), D_2^*(t), D_3^*(t)) = \min_{D_1, D_2, D_3 \in U} \{ \mathcal{J}(D_1, D_2, D_3) \}$$

corresponding to the control system (6) - (9), where $D_1 = (D_{11}, D_{12}, D_{13})$, $D_2 = (D_{21}, D_{22}, D_{23})$, $D_3 = (D_{31}, D_{33})$.

Proof. Let's consider that $\frac{dS}{dt} = f^1(t, x, D)$, $\frac{dI}{dt} = f^2(t, x, D)$ and $\frac{dB}{dt} = f^3(t, x, D)$ of the control system (6) - (9). Here $x \in X$ denotes the state variables (S, I, B) and D denote 8-tuple control variables. We take $f = (f^1, f^2, f^3)$, then clearly $X \subset \mathbb{R}^3$ and

$$f : [0, T] \times X \times U \rightarrow \mathbb{R}^3$$

is a continuous function of t and x for each $D_{ij} \in U$. Now we have to show (F1) – (F3) of *Theorem 2.2* of [30] hold true.

F1: Here each f^i 's have the continuous and bounded partial derivatives which imply that the f is Lipschitz's continuous.

F2: We consider $g_1(D_{11}, D_{21}, D_{31}) = -D_{11} - D_{12} + D_{31}$, which is bounded on U . Thus

$$\begin{aligned} \frac{f^1(t, x, D^{(1)}) - f^1(t, x, D^{(2)})}{[g_1(D^{(1)}) - g_1(D^{(2)})]} &= \frac{[D_{11}^{(2)} + D_{12}^{(2)} - D_{31}^{(2)} - D_{11}^{(1)} - D_{12}^{(1)} + D_{31}^{(1)}]S}{[D_{11}^{(2)} + D_{12}^{(2)} - D_{31}^{(2)} - D_{11}^{(1)} - D_{12}^{(1)} + D_{31}^{(1)}]} \\ &\leq \eta S = F_1(t, x) \\ \therefore f^1(t, x, D^{(1)}) - f^1(t, x, D^{(2)}) &\leq F_1(t, x) \bullet [g_1(D^{(1)}) - g_1(D^{(2)})] \end{aligned}$$

Here $\eta > 1$ is a real number. Moreover since U compact and g_1 is continuous we have $g_1(U)$ to be compact. Also since the function $g_1(U)$ is linear so the range of g_1 i.e. $g_1(U)$ will be convex. Since U is non-negative so g_1^{-1} is non-negative.

Similarly for $f^2(t, x, D)$ we can choose $g_2(D_{12}, D_{22}) = -D_{12} - D_{22}$ and $F_2(t, x) = I$ and prove F2 in a similar way.

Now for $f^3(t, x, D)$ we have to choose $g_3(D_{23}, D_{33}) = -D_{23}^2 - D_{33}$

$$\begin{aligned} \frac{f^2(t, x, D^{(1)}) - f^2(t, x, D^{(2)})}{[g_2(D^{(1)}) - g_2(D^{(2)})]} &= \frac{[D_{23}^{2(2)} + D_{33}^{(2)} - D_{23}^{2(1)} - D_{33}^{(1)}]I - [D_{13}^{2(1)} - D_{13}^{2(2)}]B}{[D_{23}^{2(2)} + D_{33}^{(2)} - D_{23}^{2(1)} - D_{33}^{(1)}]} \\ &\leq \frac{[D_{23}^{2(2)} + D_{33}^{(2)} - D_{23}^{2(1)} - D_{33}^{(1)}]I}{[D_{23}^{2(2)} + D_{33}^{(2)} - D_{23}^{2(1)} - D_{33}^{(1)}]} = I = F_3(t, x) \left(\text{provided } D_{13}^{2(1)} \geq D_{13}^{2(2)} \right) \\ \therefore f^3(t, x, D^{(1)}) - f^3(t, x, D^{(2)}) &\leq F_3(t, x) \bullet [g_3(D^{(1)}) - g_3(D^{(2)})] \end{aligned}$$

F3: Since S, I, B are bounded on $[0, T]$ so $F(\bullet, x^u) \in \mathcal{L}_1$

Now we have to show that the running cost function

$$C(t, x, D) = I(t) + B(t) + P[D_{11}^2(t) + D_{12}^2(t) + D_{13}^3(t)] + Q[D_{21}^2(t) + D_{22}^2(t) + D_{23}^3(t)] + R[|D_3(t)|^2]$$

satisfies the conditions (C1) – (C5) of *Theorem 2.2* of [30]. Here $C : [0, T] \times X \times U \rightarrow \mathbb{R}$

C1: Here $C(t, \bullet, \bullet)$ is a continuous function as it is sum of continuous functions which are functions of $t \in [0, T]$.

C2: Since a S, I and B and all D_{ij} 's are bounded implying that $C(\bullet, x, D)$ is bounded and hence measurable for each $x \in X$ and $D_{ij} \in U$.

C3: Consider $\Psi(t) = \kappa$ such that $\kappa = \min\{I(0), B(0)\}$ then Ψ will be bounded such that for all $t \in [0, T]$, $x \in X$ and $D_{ij} \in U$ we have

$$C(t, x, D) \geq \Psi(t)$$

C4: Since $C(t, x, D)$ is sum of the function which are convex in U for each fixed $(t, x) \in [0, T] \times X$ therefore $C(t, x, D)$ follows the same.

C5: Using similar type of argument we can easily show that for each fixed $(t, x) \in [0, T] \times X$, $C(t, x, D)$ is a monotonically increasing function.

Hence we have shown that the optimal control problem satisfies the all hypothesis of the *Theorem 2.2* of [30]. Therefore there exists a 8- tuple of optimal controls $(D_1^*(t), D_2^*(t), D_3^*(t))$ in the set of admissible controls U such that the cost function is minimized. \square

7.3 Characteristics for the optimal control

In this section we obtain the characteristics of the optimal control using the *Pontryagin's Maximum Principle* [31].

The Hamiltonian for the system (6) - (9) is given by

$$H(I, V, D_1, D_2, D_3, \lambda) = I(t) + B(t) + P[D_{11}^2(t) + D_{12}^2(t) + D_{13}^3(t)] + Q[|D_2|^2] + R[|D_3|^2] + \lambda_1 \frac{dS}{dt} + \lambda_2 \frac{dI}{dt} + \lambda_3 \frac{dB}{dt} \quad (11)$$

where $\lambda = (\lambda_1, \lambda_2, \lambda_3)$ is the co-state vector or adjoint vector. Now the canonical equations that relates state variable and co state variable are given by

$$\begin{aligned} \frac{d\lambda_1}{dt} &= -\frac{\partial H}{\partial S} \\ \frac{d\lambda_2}{dt} &= -\frac{\partial H}{\partial I} \\ \frac{d\lambda_3}{dt} &= -\frac{\partial H}{\partial B} \end{aligned} \quad (12)$$

Now substituting the value of the Hamiltonian the above equation we get

$$\begin{aligned} \frac{d\lambda_1}{dt} &= (\beta B + \mu_1 + \gamma + D_{11} + D_{21} - D_{31})\lambda_1 - (\beta B)\lambda_2 \\ \frac{d\lambda_2}{dt} &= (\mu_1 + \delta + D_{12} + D_{22})\lambda_2 - (\alpha - D_{23}^2 - D_{33})\lambda_3 - 1 \\ \frac{d\lambda_3}{dt} &= (\beta S)\lambda_1 - (\beta S)\lambda_2 + (y + \mu_2 + D_{13}^2)\lambda_3 - 1 \end{aligned} \quad (13)$$

along with the transversality condition $\lambda_1(T) = 0$, $\lambda_2(T) = 0$ and $\lambda_3(T) = 0$. Now using the fact that at optimal controls, $D_{ij} = D_{ij}^*$ and the value of Hamiltonian is minimum implying that $\frac{\partial H}{\partial D_{ij}} = 0$ at $D_{ij} = D_{ij}^*$ for $1 \leq i, j \leq 3$ and $ij \neq 32$, and solving (7.7) we have the following values for the optimal controls.

$$\begin{aligned} D_{11}^* &= \min \left\{ \max \left\{ \frac{S\lambda_1}{2P}, 0 \right\}, D_{11} \max \right\} \\ D_{12}^* &= \min \left\{ \max \left\{ \frac{I\lambda_2}{2P}, 0 \right\}, D_{12} \max \right\} \\ D_{13}^* &= \min \left\{ \max \left\{ \frac{2I\lambda_3}{3P}, 0 \right\}, D_{13} \max \right\} \\ D_{21}^* &= \min \left\{ \max \left\{ \frac{S\lambda_1}{2Q}, 0 \right\}, D_{21} \max \right\} \\ D_{22}^* &= \min \left\{ \max \left\{ \frac{I\lambda_2}{2Q}, 0 \right\}, D_{22} \max \right\} \\ D_{23}^* &= \min \left\{ \max \left\{ \frac{2B\lambda_3}{3Q}, 0 \right\}, D_{23} \max \right\} \end{aligned}$$

$$D_{31}^* = \min \left\{ \max \left\{ \frac{-S\lambda_1}{2R}, 0 \right\}, D_{31}^{max} \right\}$$

$$D_{33}^* = \min \left\{ \max \left\{ \frac{I\lambda_2}{2R}, 0 \right\}, D_{33}^{max} \right\}$$

7.4 Numerical Studies for the Optimal Control Problem with MDT

In this section we numerically obtain the optimal drug regimen for the control problem (6) - (9) using the optimal controls obtained in the earlier section.

For the numerical simulations we consider a time period of 100 days ($T = 100$) and the parameter values are chosen as $\omega = 20.9$, $\beta = 0.03$, $\mu_1 = 0.00018$, $\gamma = 0.01795$, $\delta = 0.2681$, $\alpha = 0.2$, $y = 0.3$ and $\mu_2 = 0.57$. First we have solved the system numerically without any drug intervention. All the numerical calculation were done in MATLAB and we used 4th order Runge-Kutta method to solve system of ODEs. Here we consider the initial value of the state variables as $S(0) = 520$, $I(0) = 275$ and $B(0) = 250$ as in [6].

Further to simulate the system with controls, we use the Forward-backward sweep method starting with the initial value of the controls as zero and estimate the state variables forward in time. Since the transversality conditions have the value of adjoint vector at end time T , so the adjoint vector was calculated backward in time.

Using the value of state variables and adjoint vector we calculate the control variables at each time instance that get updated in each iteration. We continue this till the convergence criterion is met [32].

The weights P, Q and R in the cost function \mathcal{J}_{min} are chosen based on their *hazard ratio* of the corresponding drugs. We chose the weights directly proportional to the hazard ratios. In Table 5 the hazard ratios of the different drugs are enlisted. We have chosen the weights (P, Q and S) proportional to the hazard ratios i.e. $P = 1$, $Q = 1.99$ and $R = 7.1$.

Drugs	Hazard Ratio	Source
Rifampin	0.26	[33]
Dapsone	0.99	[34]
Clofazimine	1.85	[34]

Table 5: Hazard Ratio of the drugs

We now numerically simulate the S, I and B populations without control interventions, with single control intervention, with two control interventions and finally with three control interventions of MDT.

The Figure 10 depicts the dynamics of the S, I and B populations without any control/drug interventions

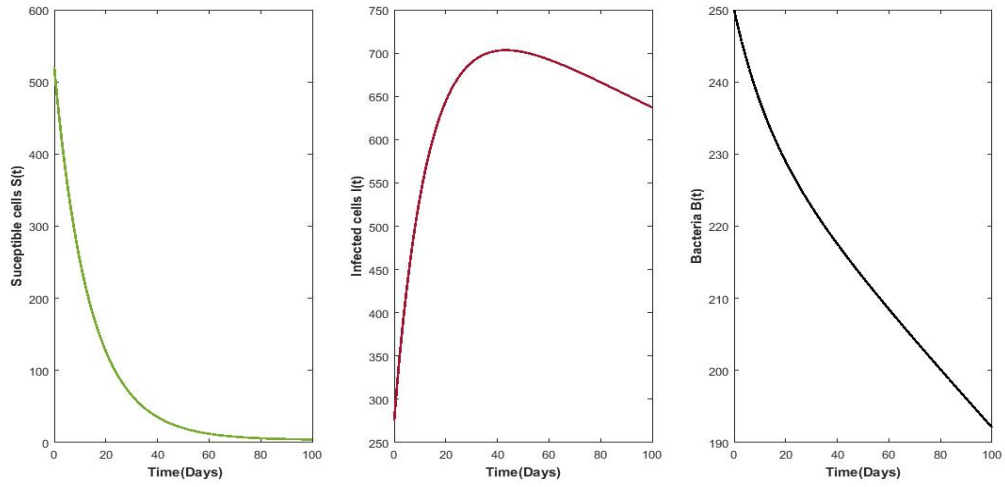


Figure 10: Plots depicting the S, I and B populations without any control interventions

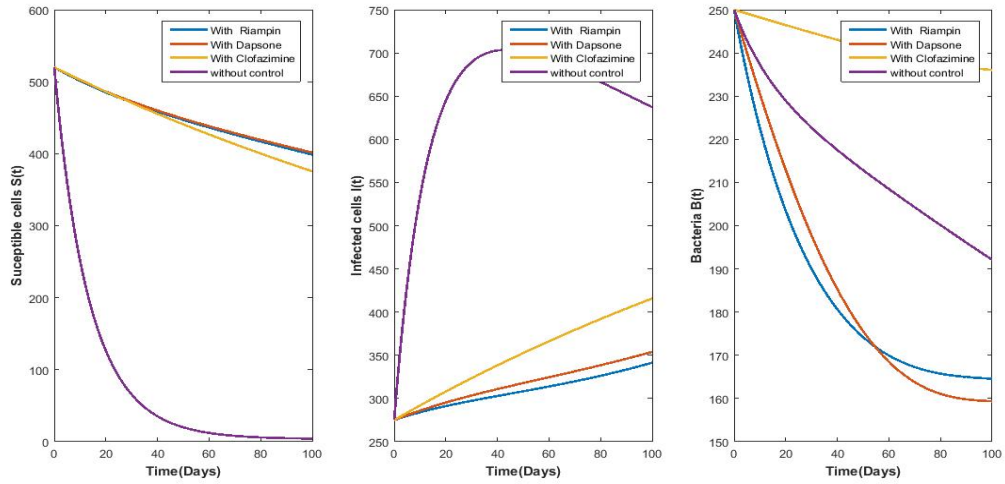


Figure 11: Plots depicting the dynamics of the S, I and B populations when one drug is introduced

The plot 11 illustrate that when individually drugs are administered the susceptible cell count decrease and the opposite effect is seen for infected cells and bacterial load compartments. One notable thing is there that the clofazimine alone can't decrease the bacterial load in the long run. Figure 12 shows that the combination of two drugs are more effective than one drug given at a time. As earlier here as we see the susceptible cell count decrease and increase in both the infected cells and bacterial load compartments.

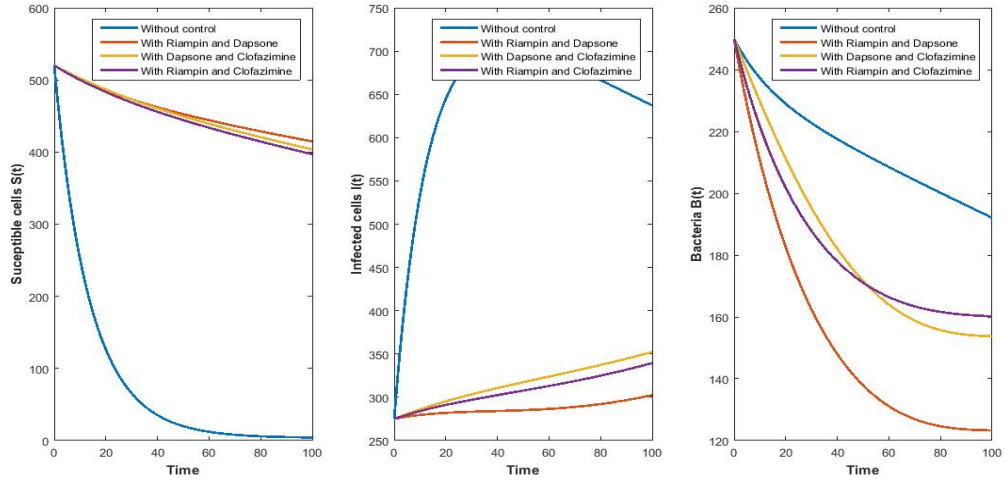


Figure 12: Plots depicting the dynamics of the S, I and B populations when combination of two drug is introduced

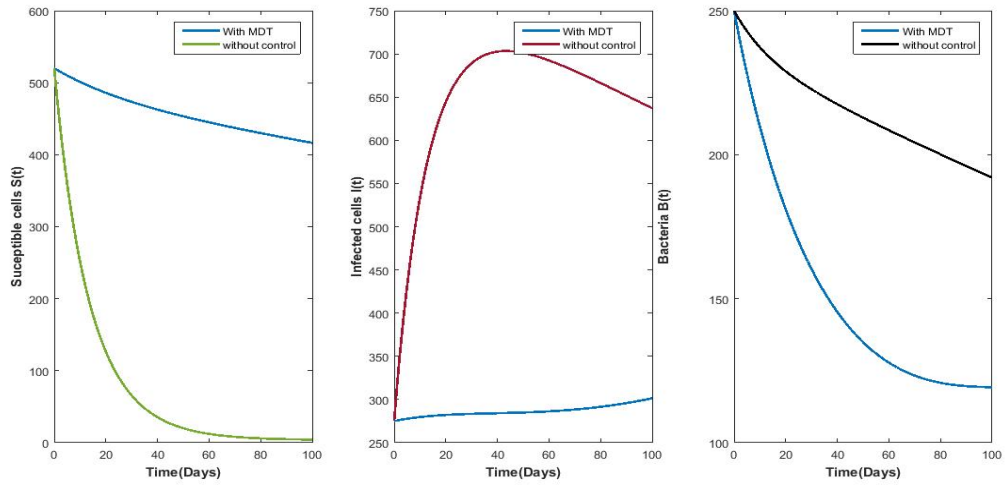


Figure 13: Plots depicting the dynamics of the the S, I and B populations with MDT intervention

The Figure 13 shows the dynamics of the S, I and B populations with MDT intervention whose findings are in similar lines to earlier two plots.

The following Table 6 gives the average S, I and B cell count for single drug, two drug combination and MDT scenarios. From the table it can be seen that MDT is the best and optimal combination for achieving the optimal increase in susceptible cells and optimal decrease in both infected cells and bacterial load.

Drug Combination	Avg susceptible cells	Avg Infected cells	Avg Bacterial load
Rifampin	450.845778	308.544767	184.353265
Dapsone	452.654249	316.861762	185.826321
Clofazimine	443.133511	350.173515	241.995028
Rifampin and Dapsone	457.141441	286.714732	153.050429
Rifampin and Clofazimine	453.456572	316.303543	182.278864
Dapsone and Clofazimine	448.689818	307.856580	181.470695
MDT	457.899776	286.431294	150.360779

Table 6: Average count of the S, I and B cells for single drug, two drug combination and MDT scenarios

7.5 Optimal control problem associated with MDT along with steroids

Corticosteroid is a steroid which is mainly used for protecting the nerve damage by suppressing the cytokines responses caused due to presence of *M. leprae* [35]. Corticosteroid is usually given after some days of MDT drugs. To capture this aspect we introduce a time delay τ in the MDT control. In others words we consider D'_{ij} s at $(t - \tau)$ and consider the control associated with steroid as $C(t)$.

With the above modifications, the set of controls now is given by

$$U = \left\{ D_{ij}(t) : D_{ij}(t) \in [0, D_{ij}max], C(t) \in [0, Cmax] 1 \leq i, j \leq 3, ij \neq 32, t \in [0, T] \right\}$$

and the modified objective function and control system is given by

$$\begin{aligned} \mathcal{J}_{min}(D_1, D_2, D_3) = & \int_0^T \left(I(t) + B(t) + P[D_{11}^2(t - \tau) + D_{12}^2(t - \tau) + D_{13}^3(t - \tau)] \right. \\ & \left. + Q[D_{21}^2(t - \tau) + D_{22}^2(t - \tau) + D_{23}^3(t - \tau)] + R[|D_3(t - \tau)|^2] + TC^2(t) \right) dt \end{aligned} \quad (14)$$

$$\frac{dS}{dt} = \omega - \beta SB - \gamma S - \mu_1 S - D_{11}(t - \tau)S - D_{21}(t - \tau)S + D_{31}(t - \tau)S + C(t)S \quad (15)$$

$$\frac{dI}{dt} = \beta SB - \delta I - \mu_1 I - D_{12}(t - \tau)I - D_{22}(t - \tau)I \quad (16)$$

$$\frac{dB}{dt} = (\alpha - D_{23}^2(t - \tau) - D_{33}(t - \tau))I - yB - \mu_2 B - D_{13}^2(t - \tau)B \quad (17)$$

Here the the Lagrangian is the integrand of the cost function (14) and is given by

$$\begin{aligned} L(I, V, D_1, D_2, D_3, C) = & \left(I(t) + B(t) + P[D_{11}^2(t - \tau) + D_{12}^2(t - \tau) + D_{13}^3(t - \tau)] \right. \\ & \left. + Q[D_{21}^2(t - \tau) + D_{22}^2(t - \tau) + D_{23}^3(t - \tau)] + R[|D_3(t - \tau)|^2] + TC^2(t) \right) \end{aligned} \quad (18)$$

The admissible set of solutions for the above optimal control problem will now lie in the set

$$\Omega = \left\{ (I, V, D_1, D_2, D_3, C) : I, V \text{ satisfy (7) - (9)} \forall (D_1, D_2, D_3, C) \in U \right\}$$

The existence of the optimal control can be shown in the similar way as it was shown in the previous optimal control problem in the preceding section.

We see that the Hamiltonian for the system (14) - (17) is given by

$$H(I, V, D_1, D_2, D_3, \lambda) = L(I, V, D_1, D_2, D_3, C) + \lambda_1 \frac{dS}{dt} + \lambda_2 \frac{dI}{dt} + \lambda_3 \frac{dB}{dt} \quad (19)$$

where $\lambda = (\lambda_1, \lambda_2, \lambda_3)$ is the co-state vector or adjoint vector. Now the *canonical equations* that relates state variable and co state variable are given by

$$\begin{aligned} \frac{d\lambda_1}{dt} &= -\frac{\partial H}{\partial S} \\ \frac{d\lambda_2}{dt} &= -\frac{\partial H}{\partial I} \\ \frac{d\lambda_3}{dt} &= -\frac{\partial H}{\partial B} \end{aligned} \quad (20)$$

Now substituting the value of the Hamiltonian in the above equation we get

$$\begin{aligned} \frac{d\lambda_1}{dt} &= (\beta B + \mu_1 + \gamma + D_{11}(t - \tau) + D_{21}(t - \tau) - D_{31}(1 - \tau) - C(t))\lambda_1 - (\beta B)\lambda_2 \\ \frac{d\lambda_2}{dt} &= (\mu_1 + \delta + D_{12}(t - \tau) + D_{22}(t - \tau))\lambda_2 - (\alpha - D_{23}^2(t - \tau) - D_{33}(t - \tau))\lambda_3 - 1 \\ \frac{d\lambda_3}{dt} &= (\beta S)\lambda_1 - (\beta S)\lambda_2 + (y + \mu_2 + D_{13}^2(t - \tau))\lambda_3 - 1 \end{aligned} \quad (21)$$

along with the transversality condition $\lambda_1(T) = 0$, $\lambda_2(T) = 0$ and $\lambda_3(T) = 0$.

We now have $\frac{\partial H}{\partial D_{ij}} = 0$ and $\frac{\partial H}{\partial C} = 0$ at $D_{ij} = D_{ij}^*$ and $C = C^*$ for $1 \leq i, j \leq 3$ and $ij \neq 32$.

Now differentiating the Hamiltonian and solving it for D_{ij}^* and C^* we have the values for the optimal controls as

$$\begin{aligned} D_{11}^*(t - \tau) &= \min \left\{ \max \left\{ \frac{S\lambda_1}{2P}, 0 \right\}, D_{11} \max \right\} \\ D_{12}^*(t - \tau) &= \min \left\{ \max \left\{ \frac{I\lambda_2}{2P}, 0 \right\}, D_{12} \max \right\} \\ D_{13}^*(t - \tau) &= \min \left\{ \max \left\{ \frac{2I\lambda_3}{3P}, 0 \right\}, D_{13} \max \right\} \\ D_{21}^*(t - \tau) &= \min \left\{ \max \left\{ \frac{S\lambda_1}{2Q}, 0 \right\}, D_{21} \max \right\} \\ D_{22}^*(t - \tau) &= \min \left\{ \max \left\{ \frac{I\lambda_2}{2Q}, 0 \right\}, D_{22} \max \right\} \\ D_{23}^*(t - \tau) &= \min \left\{ \max \left\{ \frac{2B\lambda_3}{3Q}, 0 \right\}, D_{23} \max \right\} \\ D_{31}^*(t - \tau) &= \min \left\{ \max \left\{ \frac{-S\lambda_1}{2R}, 0 \right\}, D_{31} \max \right\} \end{aligned}$$

$$D_{33}^*(t - \tau) = \min \left\{ \max \left\{ \frac{I\lambda_2}{2R}, 0 \right\}, D_{33}^{max} \right\}$$

$$C^*(t) = \min \left\{ \max \left\{ \frac{S\lambda_1}{2T}, 0 \right\}, D_{33}^{max} \right\}$$

7.5.1 Numerical simulations for Optimal Control with both MDT and Steroids

Here we use all the parameter values and initial conditions same as in the previous optimal control problem. The value of the weight T was chosen to be 6.4230 based on the hazard ratio value 1.67 [34]. Instead of forward backward sweep we use only forward sweep for calculating the state variables and adjoint vectors after the delay τ . Here we considered $\tau = 55$ days and the step size as $h = 0.0000045$.

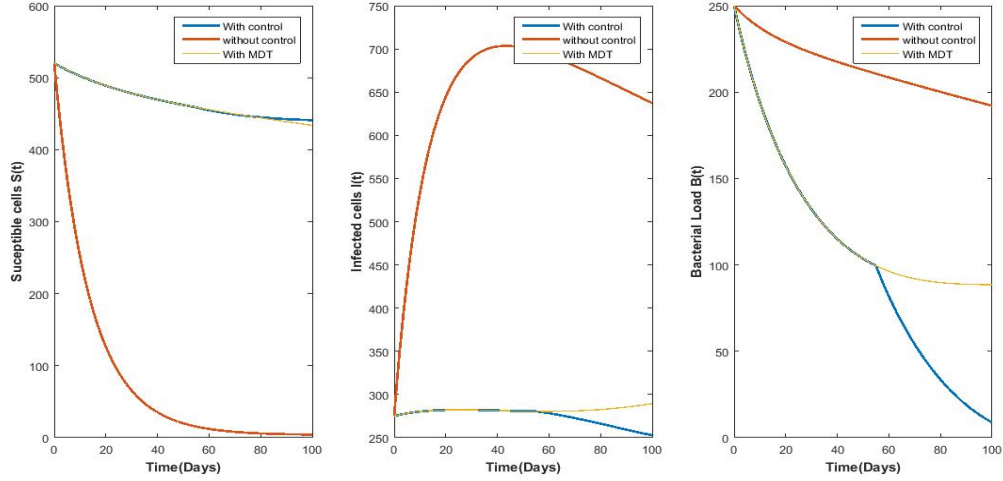


Figure 14: Plots depicting the system dynamics when MDT and steroids are intervened.

From the Figure 14 it can be seen that the combined combination of MDT and corticosteroid seems to be doing the best job in decreasing the lepra type 1 reaction disease burden.

8 Comparative and Effectiveness Study

In this section we will perform the comparative and effectiveness study for the system (7) - (9).

For this system without any control/drug interventions the basic reproduction number is given by

$$\mathcal{R}_0 = \frac{\alpha\beta\omega}{(\gamma + \mu_1)(\delta + \mu_1)(y + \mu_2)}$$

Now to study the effectiveness of each of these control/drug interventions we calculate the modified reproduction number $\overline{\mathcal{R}_0}$ based on the modified parameters which gets altered owing to these interventions as follows:

- The drug dapsone primarily acts on the inhibition of viral replication. Based on this we consider α to be $\alpha(1 - \epsilon)$ where ϵ denotes the efficiency of the drug dapsone.
- Since the drug rifampin is a killer of bacteria it indirectly reduces the interaction between susceptible cells and the bacteria. Owing to this we choose β as $\beta(1 - \rho)$ where ρ denotes the efficacy of rifampin in killing bacteria.
- The drug clofazimine primarily inhibits the cytokines responses indirectly reducing the death of healthy cells. Owing to this we consider γ to be $\frac{\gamma}{(1-c)}$ where c denotes the efficacy of clofazimine in suppressing cytokines responses.

With the above modified parameters based on the action of control/drug interventions, we get the modified reproduction number $\overline{\mathcal{R}_0}$ as

$$\overline{\mathcal{R}_0} = \frac{\alpha(1 - \epsilon)\beta(1 - \rho)\omega}{\left(\frac{\gamma}{1 - c} + \mu_1\right)(\delta + \mu_1)(y + \mu_2)}$$

We now do the comparative and effectiveness study by calculating the percentage of reduction \mathcal{R}_0 with reference to modified $\overline{\mathcal{R}_0}$ as follows:

$$\text{Percentage of reduction in } \mathcal{R}_0 = \left[\frac{\mathcal{R}_0 - \overline{\mathcal{R}_0}}{\mathcal{R}_0} \right] \times 100$$

We do this study for different efficacy levels of the drugs such as

(a) Low Efficacy (LE) given by 0.3 (b) Medium Efficacy (ME) given by 0.6 and (c) High Efficacy (HE) given by 0.9.

In the following table the comparative and effectiveness study is done and the the drug combinations are ranked based on the reduction in percentage of \mathcal{R}_0 for different efficacy levels of the drugs. The highest rank is given for the drug combination that has highest reduction in the reproduction number. The efficacy at different levels were chosen with rifampin taken as the base value and the efficacy of dapsone and clofazimine were taken lesser than this based on their hazard ratios using the fact that higher the hazard ratio lower the efficacy level.

Sl No	Drug Combination	%age LE	Rank	%age ME	Rank	%age HE	Rank
1	Rifampin	30.000000	4	60.000000	4	90.000000	4
2	Dapsone	7.880000	2	15.750000	2	23.630000	2
3	Clofazimine	0.043724	1	0.091317	1	0.143575	1
4	Rifampin and Dapsone	35.516000	6	66.300000	6	92.363000	6
5	Rifampin and Clofazimine	30.030607	5	60.036527	5	90.014357	5
6	Dapsone and Clofazimine	7.920279	3	15.826935	3	23.739648	3
7	MDT	35.544195	7	66.330774	7	92.373965	7

Table 7: Comparative and effectiveness study in terms of ranking for different combinations of drug interventions for Low efficacy (LE), Medium efficacy (ME) and High efficacy (HE)

From the above Table 7 dealing with the comparative and effectiveness study it can be seen that MDT treatment seems to be working the best in reducing the \mathcal{R}_0 percentage in comparison to single drug and two drug combinations. These findings are in line with the conclusion made for MDT interventions in section 7.4 in the optimal control setting.

9 Discussions and Conclusions

Based on the pathogenesis of leprosy in this work we have framed an deterministic model dealing with the type - I lepra reaction and the causation biomarkers . We initially studied the entire natural history of this model. The findings from this study include the following. The proposed system admits two steady dynamic states one being disease-free equilibrium and the other being the infected equilibrium. For $\mathcal{R}_0 < 1$ the system tends to stabilize around the disease free equilibrium and for $\mathcal{R}_0 > 1$ the system tends to stabilize around the infected equilibrium. The system undergoes a trans-critical bifurcation at $\mathcal{R}_0 = 1$. This developed model was validated through the 2D heat plot based on the characteristic of average doubling time of the *M.Laprae*. The sensitivity analysis using PRCC and SRCC methods showed that the burst rate of the bacteria α , is the most sensitive parameter and in case of combination of two parameters, the rate of death of infected cells due to cytokines δ , in combination with α seemed to be the most sensitive parameter combination.

After the natural history, we studied two optimal control problems the first dealing with the MDT interventions and second dealing with MDT along with steroid interventions. The findings from these studies include the following. For individual drug intervention scenario, the drug rifampin has the highest impact in reducing both the infected cells and the bacterial load. For the two drug combinations scenario, rifampin along dapsone combination was the best in reducing the disease burden. Finally we concluded that MDT combination drug intervention was the best in reducing the disease burden in comparison with single and two drug combinations. The Table 6 summarizes and justifies the above findings. Further the optimal control problem dealing with MDT along with steroid interventions also led to the conclusion that the optimal intervention is the combined intervention of administering MDT along with steroid intervention. The findings from the comparative and effectiveness study show that the drug clofazimine has the least impact in reducing the disease burden when applied individually and the drug rifampin has the highest impact. Overall MDT intervention does the best job in reducing the disease burden. The findings from the comparative and effectiveness study are in line with the observations of the optimal control studies.

This within-host modeling study of type - I lepra reaction involving the crucial biomarkers is a first of its kind. The finding from this novel and comprehensive study will help the clinicians and public health researchers in early detection of lepra reactions through study of biomarkers for prevention of subsequent disabilities.

References

- [1] W. H. Organization *et al.*, “Global consultation of national leprosy programme managers, partners and affected persons on global leprosy strategy 2021–2030: Report of the virtual meeting 26–30 october 2020.,” 2020.
- [2] O. Ojo, D. L. Williams, L. B. Adams, and R. Lahiri, “Mycobacterium leprae transcriptome during in vivo growth and ex vivo stationary phases,” *Frontiers in cellular and infection microbiology*, p. 1410, 2022.
- [3] C. Massone and E. Nunzi, “Pathogenesis of leprosy,” in *Leprosy and Buruli Ulcer*, Springer, 2022, pp. 45–48.
- [4] D. J. Blok, S. J. de Vlas, E. A. Fischer, and J. H. Richardus, “Mathematical modelling of leprosy and its control,” *Advances in Parasitology*, vol. 87, pp. 33–51, 2015.
- [5] L. Giraldo, U. Garcia, O. Raigosa, L. Munoz, M. M. P. Dalia, and T. Jamboos, “Multibacillary and paucibacillary leprosy dynamics: A simulation model including a delay,” *Appl Math Sci*, vol. 12, no. 32, pp. 1677–1685, 2018.

- [6] S. Ghosh, A. Chatterjee, P. Roy, N. Grigorenko, E. Khailov, and E. Grigorieva, “Mathematical modeling and control of the cell dynamics in leprosy,” *Computational Mathematics and Modeling*, pp. 1–23, 2021.
- [7] D. S. Ridley, *Pathogenesis of leprosy and related diseases*. Elsevier, 2013.
- [8] S. Sasaki, F. Takeshita, K. Okuda, and N. Ishii, “Mycobacterium leprae and leprosy: A compendium,” *Microbiology and immunology*, vol. 45, no. 11, pp. 729–736, 2001.
- [9] G. Weddell and E. Palmer, “The pathogenesis of leprosy,” *Lepr. Rev.*, vol. 34, p. 57, 1963.
- [10] R. P. Agarwal and D. O’Regan, *Existence and Uniqueness of Solutions of Systems*. Springer, 2008.
- [11] Y. Sibuya, P.-F. Hsieh, and Y. Sibuya, *Basic theory of ordinary differential equations*. Springer Science & Business Media, 1999.
- [12] J. M. Heffernan, R. J. Smith, and L. M. Wahl, “Perspectives on the basic reproductive ratio,” *Journal of the Royal Society Interface*, vol. 2, no. 4, pp. 281–293, 2005.
- [13] A. Korobeinikov, “Global properties of basic virus dynamics models,” *Bulletin of Mathematical Biology*, vol. 66, no. 4, pp. 879–883, 2004.
- [14] B. Buonomo, “A note on the direction of the transcritical bifurcation in epidemic models,” *Nonlinear Analysis: Modelling and Control*, vol. 20, no. 1, pp. 38–55, 2015.
- [15] H.-S. Kim, J. Lee, D. Y. Lee, Y.-D. Kim, J. Y. Kim, H. J. Lim, S. Lim, and Y. S. Cho, “Schwann cell precursors from human pluripotent stem cells as a potential therapeutic target for myelin repair,” *Stem cell reports*, vol. 8, no. 6, pp. 1714–1726, 2017.
- [16] S.-H. Jin, S.-K. An, and S.-B. Lee, “The formation of lipid droplets favors intracellular mycobacterium leprae survival in sw-10, non-myelinating schwann cells,” *PLoS neglected tropical diseases*, vol. 11, no. 6, e0005687, 2017.
- [17] R. B. Oliveira, E. P. Sampaio, F. Aarestrup, R. M. Teles, T. P. Silva, A. L. Oliveira, P. R. Antas, and E. N. Sarno, “Cytokines and mycobacterium leprae induce apoptosis in human schwann cells,” *Journal of Neuropathology & Experimental Neurology*, vol. 64, no. 10, pp. 882–890, 2005.
- [18] L. Levy and J. Baohong, “The mouse foot-pad technique for cultivation of mycobacterium leprae,” *Leprosy review*, vol. 77, no. 1, pp. 5–24, 2006.
- [19] I. L. Association *et al.*, “International journal of leprosy and other mycobacterial diseases,” 2020.
- [20] R. O. Pinheiro, J. de Souza Salles, E. N. Sarno, and E. P. Sampaio, “Mycobacterium leprae–host-cell interactions and genetic determinants in leprosy: An overview,” *Future microbiology*, vol. 6, no. 2, pp. 217–230, 2011.
- [21] K.-H. Cho, S.-Y. Shin, W. Kolch, and O. Wolkenhauer, “Experimental design in systems biology, based on parameter sensitivity analysis using a monte carlo method: A case study for the $\text{tnf}\alpha$ -mediated $\text{nf-}\kappa\text{b}$ signal transduction pathway,” *Simulation*, vol. 79, no. 12, pp. 726–739, 2003.
- [22] S. Marino, I. B. Hogue, C. J. Ray, and D. E. Kirschner, “A methodology for performing global uncertainty and sensitivity analysis in systems biology,” *Journal of theoretical biology*, vol. 254, no. 1, pp. 178–196, 2008.
- [23] X.-Y. Zhang, M. N. Trame, L. J. Lesko, and S. Schmidt, “Sobol sensitivity analysis: A tool to guide the development and evaluation of systems pharmacology models,” *CPT: pharmacometrics & systems pharmacology*, vol. 4, no. 2, pp. 69–79, 2015.
- [24] A. Saltelli, M. Ratto, T. Andres, F. Campolongo, J. Cariboni, D. Gatelli, M. Saisana, and S. Tarantola, *Global sensitivity analysis: the primer*. John Wiley & Sons, 2008.

- [25] M. B. Maymone, S. Venkatesh, M. Laughter, R. Abdat, J. Hugh, M. M. Dacso, P. N. Rao, B. M. Stryjewska, C. A. Dunnick, and R. P. Dellavalle, "Leprosy: Treatment and management of complications," *Journal of the American Academy of Dermatology*, vol. 83, no. 1, pp. 17–30, 2020.
- [26] S. L. Walker and D. N. Lockwood, "Leprosy type 1 (reversal) reactions and their management.," *Leprosy review*, vol. 79, no. 4, pp. 372–386, 2008.
- [27] K. Tripathi, *Essentials of medical pharmacology*. JP Medical Ltd, 2013.
- [28] U. Paniker and N. Levine, "Dapsone and sulfapyridine," *Dermatologic clinics*, vol. 19, no. 1, pp. 79–86, 2001.
- [29] J. C. Garrelts, "Clofazimine: A review of its use in leprosy and mycobacterium avium complex infection," *Dicp*, vol. 25, no. 5, pp. 525–531, 1991.
- [30] A. Boyarsky, "On the existence of optimal controls for nonlinear systems," *Journal of Optimization Theory and Applications*, vol. 20, no. 2, pp. 205–213, 1976.
- [31] D. Liberzon, *Calculus of variations and optimal control theory: a concise introduction*. Princeton university press, 2011.
- [32] S. Lenhart and J. T. Workman, *Optimal control applied to biological models*. Chapman and Hall/CRC, 2007.
- [33] M. I. Bakker, M. Hatta, A. Kwenang, B. H. Van Benthem, S. M. Van Beers, P. R. Klatser, and L. Oskam, "Prevention of leprosy using rifampicin as chemoprophylaxis," *The American journal of tropical medicine and hygiene*, vol. 72, no. 4, pp. 443–448, 2005.
- [34] S. R. P. S. Cerqueira, P. D. Deps, D. V. Cunha, N. V. F. Bezerra, D. H. Barroso, A. B. S. Pinheiro, G. S. Pillegi, T. A. R. Repsold, P. S. Kurizky, S. M. Collin, *et al.*, "The influence of leprosy-related clinical and epidemiological variables in the occurrence and severity of covid-19: A prospective real-world cohort study," *PLoS neglected tropical diseases*, vol. 15, no. 7, e0009635, 2021.
- [35] V. P. Shetty, F. A. Khambati, S. D. Ghate, G. D. Capadia, V. V. Pai, and R. Ganapati, "The effect of corticosteroids usage on bacterial killing, clearance and nerve damage in leprosy; part 3—study of two comparable groups of 100 multibacillary (mb) patients each, treated with mdt+steroids vs mdt alone, assessed at 6 months post-release from 12 months mdt," *Leprosy review*, vol. 81, no. 1, pp. 41–58, 2010.